Raman scattering of carbon nanotube bundles under axial strain and strain-induced debundling

Rajay Kumar and Stephen B. Cronin
Department of Electrical Engineering, University of Southern California, Los Angeles, California 90089, USA
(Received 7 January 2007; published 19 April 2007)

We measure resonant Raman scattering of individual carbon nanotube bundles under axial strains of up to 17%. The main effect of this strain is to cause debundling of the nanotubes. The *G* band Raman spectra of metallic and semiconducting nanotubes respond differently to strain and debundling, giving insight into the nature of the broad metallic G_- band line shape. For metallic nanotubes, the G_- band upshifts and becomes narrower with strain, making it appear more semiconductor-like. Surprisingly, this metal to semiconductor transition is not reversible with strain, indicating that nanotube-nanotube coupling plays a significant role in the observed G_- band of unperturbed metallic nanotubes.

DOI: 10.1103/PhysRevB.75.155421 PACS number(s): 73.61.Wp, 72.80.Rj, 78.30.Na

It is important to understand how nanotubes respond to strain, not just as a material property but also to gain insight into the behaviors of low-dimensional materials that differ fundamentally from bulk materials. Theoretical *ab initio* and tight-binding calculations predict large changes in the electronic band structure of nanotubes upon application of strain.[1–4] Conductance measurements on single wall carbon nanotubes (SWCNTs) strained by an atomic-force microscope (AFM) show an increase in resistance with strain due to localized defects,[5] mechanical deformation by the AFM tip,[6] and strain-induced band gaps.[7] While these previous studies focus on the electronic changes in nanotubes under strain, very little work has been done to determine the vibrational characteristics of nanotubes under strain. In our previous measurements, we observed large shifts in the vibrational energies of nanotubes under inhomogeneous strain as well as a characteristic difference between metallic and semiconducting nanotubes, which was not well understood theoretically.[8]

Because of the strong electron-phonon coupling in nanotubes, the *G* band Raman spectra of metallic and semiconducting nanotubes are qualitatively very different.[9] In metallic nanotubes, the lower-frequency component of the *G* band (G_-) exhibits a broad lineshape and is significantly downshifted in frequency with respect to its counterpart in semiconducting nanotubes.[10] While the G_- Raman feature in metallic nanotubes is generally attributed to phonon coupling to the continuum of electronic states, the precise nature of this feature is not understood. There have been several conflicting reports in the literature, including a Peierls-like mechanism[11,12] and a nanotube bundling effect.[13]

In this paper, we report resonant Raman spectroscopy of bundles of semiconducting and metallic SWCNTs using another method of inducing strain.[14] Our previous AFM-induced strain technique allowed Raman spectra to be taken before and after inducing strains, limited to 1.65% or less on a single nanotube.[8] Other polymeric nanotube Raman measurements focus on ensemble measurements, whereas our technique focuses on only one nanotube.[15–19] This is made possible by a lithographically defined grid pattern, which provides the high spatial precision required for single nanotube measurements. In this approach, the strain can be varied in a continuous and reversible fashion up to a maximum strain of 17% on the bundle. By establishing the reversibility of our measurements, we are able to take into account slippage of the SWCNTs on the substrate. Furthermore, we observe both reversible and irreversible changes in the Raman spectra of nanotubes in these bundles, which will be the topic of this paper.

SWCNTs synthesized by the laser ablation method[20] are sonicated in an isopropyl alcohol solution for 20 min and then deposited onto a 1 mm thick film of polydimethyl siloxane (PDMS) created from a Sylgard 184 silicone elastomer kit (Corning, Inc.). Metal strips of Cr-Au, patterned on top of the SWCNTs using photolithography, serve to hold the ends of the bundle fixed to the PDMS substrate. An AFM image of these strips holding a SWCNT bundle is shown in Fig. 1(a). The ends of the PDMS substrate are then clamped and the entire substrate is strained along its length. The amount of strain is determined by dividing the increase in length between predefined grid markers by the unstrained length and then multiplying by the cosine of the angle between the nanotube and direction of strain. AFM images are taken to ensure that both ends of the nanotube are pinned beneath the strips and to determine the angle between the nanotube and the direction of the applied strain. Raman spectra are taken with a Renishaw *inVia* Raman microprobe with a 532 nm Spectra Physics solid-state laser and 633 nm HeNe laser, each delivering 1–2 mW of power. The Raman spectra are taken as the PDMS substrate is incrementally strained and unstrained.

The nanotube bundle shown in Fig. 1 has a diameter of 13 nm and is expected to contain approximately 60 single wall nanotubes. It is likely the case that several nanotubes contribute to the *G* band spectrum, while only one nanotube contributes to the radial breathing mode (RBM) spectrum. The RBM frequency (ω_{RBM}) for the resonant nanotube in Fig. 1 is 196 cm^{-1}, implying a diameter (d_t) of 1.3 nm by the relation $\omega_{\mathrm{RBM}}=A/d_t+B$, where $A=223.5\ \mathrm{cm}^{-1}\ \mathrm{nm}$ and $B=12.5\ \mathrm{cm}^{-1}$.[21] Figure 1 shows the frequency of the *G* band Raman mode of this SWCNT bundle at various degrees of strain. The Raman spectrum's sharp *G* band line shape (upper right inset) indicates its semiconducting nature.[22] During the initial 3% of strain, there is no change in the Raman frequency, indicating that the nanotube bundle is still slack between the metal strips. Beyond 3%, the *G* band frequency

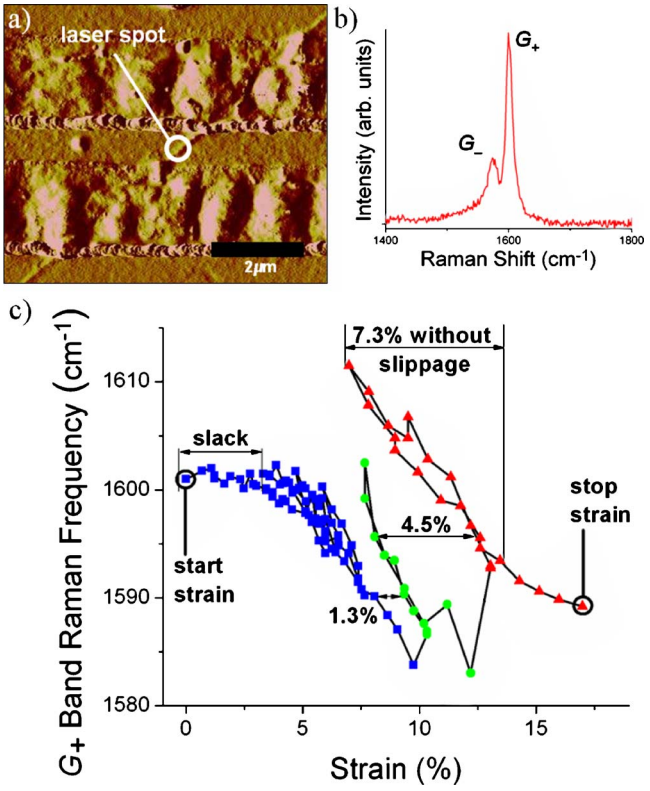

FIG. 1. (Color online) (a) AFM image of a carbon nanotube bundle pinned under gold strips with a 0.5 μm diameter laser spot. The scale bar is 2 μm. (b) Raman spectrum from a 532 nm laser taken at 0% strain. The sharp peaks are typical of semiconducting nanotubes and show the high-frequency component G_+ and lower-frequency component G_-. (c) G_+ Raman frequency plotted as a function applied strain. Note the reversible regions of the strain, separated by discrete slips of 1.3% and 4.5%.

downshifts at a rate of 2.9 cm^{-1}/% strain. After reaching a strain of 6.5%, the strain is reduced to 4.7% in order to demonstrate that the strain is not relaxing due to slippage underneath the Cr-Au strips. The strain is then increased and decreased twice to ensure that the G band frequency varies reversibly before increasing to 10% strain and beyond. Above 10% strain, we see a discrete jump in the Raman frequency of this nanotube, indicating a slip in strain of 1.3%. Similarly, we see another discrete jump of 4.5% at 13% strain. In between these discrete "jumps," the frequency versus strain relationship is found to be reversible, indicating no slippage. We observe similar downshifts of the D, G, and G' bands of this semiconducting nanotube. Ultimately, the PDMS substrate broke when 17% strain was achieved on the nanotube bundle. Figure 1 shows typical results that were observed consistently in a total of four semiconducting nanotubes measured with this technique.

Although we were able to achieve 7.3% strain without slippage of the bundle, twisting and sliding of the nanotubes within the bundle account for a majority of the bundle elongation,[23] resulting in a significantly reduced actual strain on each individual nanotube. By comparing the large strain-induced downshifts observed in our previous work (14.8 cm^{-1} downshift at 0.5% strain) with the relative small downshifts observed in this work (2.9 cm^{-1}/% strain), we estimate the actual strain on the individual nanotubes within the bundle to be a factor of 10 lower than the nominal strain on the bundle.[24] This implies that the strain-induced changes in the optical transition energies are ten times less than the 100 meV predicted theoretically for carbon nanotubes under these high strains and therefore remain well within the resonant window.[1,2] The relative intensity of the D band divided by that of the G band (I_D/I_G) is a quantity that increases as the sp^2 symmetry of a nanotube is broken. In our measurements, I_D/I_G was not observed to change under applied strain. This is surprising considering the large amount of strain applied (7.3%), which is expected to induce a significant distortion of the graphitic hexagons to break the sp^2 symmetry. The lack of change in I_D/I_G, together with the very small strain-induced downshift of the G band ($\Delta\omega_G/\Delta\sigma=2.9\%$), indicates that there is significant sliding of the nanotubes along each other within the bundle that distribute the nominal strain to the entire bundle. This results in a significantly reduced strain on each individual nanotube within the bundle.[25,26]

Changes in the RBM frequency of the metallic nanotubes (not shown) corroborate the strain-induced debundling phenomenon. The RBM was observed to shift up irreversibly by ~4 cm^{-1} with applied strain. This irreversible upshift was found consistently in a total of four metallic nanotubes and three semiconducting nanotubes measured using this PDMS strain technique. This result agrees with the previous experimental findings of Rao *et al.*, who found the RBM frequencies of individual nanotubes to be slightly increased from those of nanotube bundles and attributed it to decoupling rather than a change in diameter.[27]

Figure 2 shows the frequency of the upper (G_+) and lower (G_-) components of the G band Raman mode of a different SWCNT bundle measured at various degrees of strain with 633 nm light. The broad and downshifted G_- peak indicates that the resonant nanotube in the bundle is metallic.[28] The Raman frequency of the G_+ mode varies reversibly with strain, while the G_- mode varies irreversibly. The data start at 8.4% strain. As the strain was decreased to 7.5%, the G_- mode shifted up from 1558 to 1567 cm^{-1}, while the G_+ mode shifted up by only 2 cm^{-1}. The strain was subsequently increased to 11.3%, resulting in a downshift of both the G_+ and G_- modes. Here, the G_+ mode shifts reversibly, and the G_- mode shifts irreversibly. After 12%, the strain was reduced. Again, the G_+ mode varies reversibly along the same slope, while the G_- mode increases rapidly in an irreversible fashion. All subsequent straining resulted in reversible shifts of both G_+ and G_- modes, with average slopes of −1.8 strain and −0.9 cm^{-1}/% strain, respectively. These reversible downshifts with strain are understood on the basis of the elongation of the C–C bond, which weakens the bond therefore lowering its vibrational frequency.

The straining and relaxing of the nanotube shown in Fig. 2 resulted in an overall upshift of the G_- band by 20 cm^{-1} from 1558 to 1578 cm^{-1}. This irreversible upshift can be seen clearly in Figs. 2(b) and 2(c). The pronounced upshift was observed consistently in all four metallic nanotubes

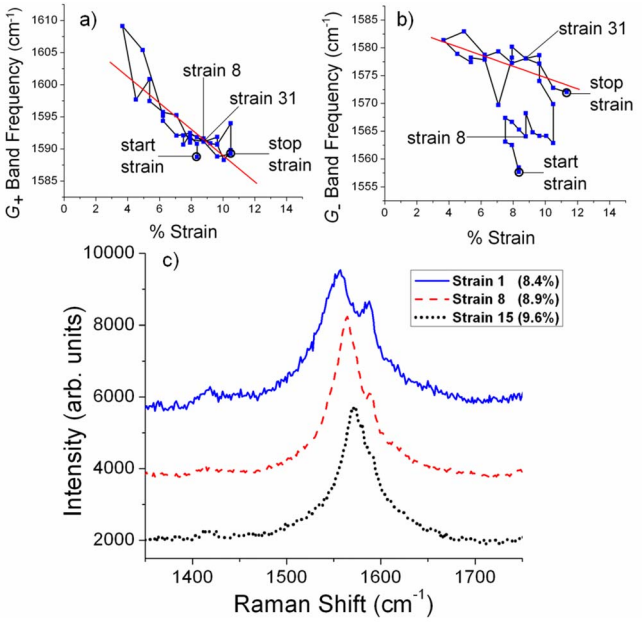

FIG. 2. (Color online) (a) G_+ band and (b) G_- band Raman frequencies of one of four metallic nanotubes at various degrees of strain. (c) G band Raman spectra taken by a 633 nm laser after subsequent straining and unstraining of the bundle.

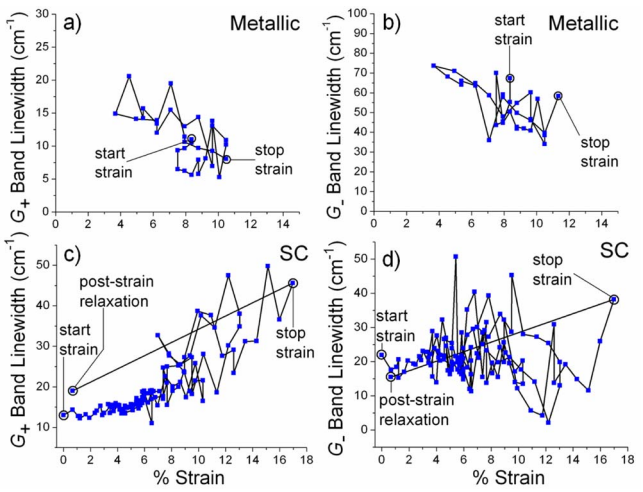

FIG. 3. (Color online) (a) G_+ band and (b) G_- band FWHM linewidths for a metallic nanotube measured with a 633 nm laser and (c) G_+ band and (d) G_- band FWHM linewidths for a semiconducting nanotube measured with a 532 nm laser.

measured in this study but was not observed in any of the semiconducting nanotubes measured. We attribute this upshift to a change in the nanotube-nanotube coupling within this bundle, which affects this Raman mode through plasmon-phonon coupling. That is, the G_- band phonons of the resonant nanotube couple to plasmons in neighboring nanotubes within the bundle. This plasmon-phonon coupling mechanism has been predicted to cause phonon softening (downshift) of the G band in metallic nanotubes.[6] The irreversible upshifts observed under strain indicate that the plasmonic coupling of neighboring nanotubes is weakened as the bundle is perturbed (strained or relaxed), thereby causing an upshift of the G_- Raman mode.

After the nanotubes cease decoupling with strain, we see reversible changes in the G band linewidths. We observe a difference in the reversible changes of metallic and semiconducting nanotubes. Figure 3 shows the G band linewidths (full width at half maximum) plotted as a function of strain for a metallic and a semiconducting nanotube. It is clear from this figure that metallic and semiconducting nanotubes respond very differently to strain. The G band linewidths of semiconducting nanotubes increase with strain [Figs. 3(c) and 3(d)], while those of metallic nanotubes decrease with strain [Figs. 3(a) and 3(b)]. The strain-induced broadening observed in semiconducting nanotubes is attributed to inhomogeneity, which is expected if the strain is not uniformly distributed along the length of the nanotube. The strain-induced narrowing we observe in the case of the metallic nanotubes is very different from this broadening and indicates the presence of a fundamentally different phenomenon. The reversible change in the linewidth of metallic nanotubes indicates that this effect is related to the formation of a strain-induced band gap. Unlike nanotube-nanotube coupling, the strain-induced band gap varies reversibly with strain. The strain-induced band gap changes the number of free carriers at the Fermi energy, which strongly interact with this phonon mode. The G_- band FWHM data shown in Fig. 3(b) was fit to a slope of -4 cm^{-1}/% strain. It is difficult to estimate the change in the band gap with strain because the actual strain on each individual nanotube is much less than the nominal strain on the bundle.

In conclusion, the resonant Raman spectra of nanotube bundles were measured under strains of up to 17%. The elastic polymer substrate technique allows the strain to be varied in a reversible fashion over a wide range of strains. We find that only a small fraction of the strain applied to the bundle is transferred to individual nanotubes within the bundle. The main effect of this strain is to debundle the nanotubes. The G band Raman frequency is found to decrease with applied strain due to the elongation of the C–C bond. Slippage of the nanotubes on the substrate is found to occur in discrete jumps and can therefore be determined quantitatively from the Raman data. As the nanotube bundles are strained, their RBM frequencies increase, indicating a strain-induced decoupling of nanotubes within the bundle. The G_+ band Raman frequency decreases by $\sim$15 cm^{-1} for both metallic and semiconducting nanotubes over the applied strain range. However, the G_- band Raman spectra of metallic and semiconducting nanotubes respond differently to strain, giving insight into the nature of the broad metallic G_- band lineshape. The G_- band frequency decreases by $\sim$15 cm^{-1} with applied strain for semiconducting nanotubes, while the G_- band is found to increase by 20 cm^{-1} and becomes more narrow with strain for metallic nanotubes. However, this upshift is not reversible with strain, indicating that nanotube-nanotube decoupling is the main cause of the observed changes in the broad G_- band line shape of metallic nanotubes.

[1] R. Heyd, A. Charlier, and E. McRae, Phys. Rev. B **55**, 6820 (1997).
[2] L. Yang, M. P. Anantram, J. Han, and J. P. Lu, Phys. Rev. B **60**, 13874 (1999).
[3] T. Ito, K. Nishidate, M. Baba, and M. Hasegawa, Surf. Sci. **514**, 222 (2002).
[4] S. Ogata and Y. Shibutani, Phys. Rev. B **68**, 165409 (2003).
[5] D. Bozovic, M. Bockrath, J. H. Hafner, C. M. Leiber, H. Park, and M. Tinkham, Phys. Rev. B **67**, 033407 (2003).
[6] T. W. Tombler, C. Zhou, L. Alexseyev, J. Kong, H. Dai, L. Liu, C. S. Jayanthi, M. Tang, and S.-Y. Wu, Nature (London) **405**, 769 (2000).
[7] E. D. Minot, Y. Yaish, V. Sazonova, J.-Y. Park, M. Brink, and P. L. McEuen, Phys. Rev. Lett. **90**, 156401 (2003).
[8] S. B. Cronin, A. K. Swan, M. S. Ünlü, B. B. Goldberg, M. S. Dresselhaus, and M. Tinkham, Phys. Rev. B **72**, 035425 (2005).
[9] M. S. Dresselhaus, G. Dresselhaus, A. Jorio, A. G. Souza Filho, and R. Saito, Carbon **40**, 2043 (2002).
[10] F. Wang, M. Y. Sfeir, L. Huang, X. M. Henry Huang, Y. Wu, J. Kim, J. Hone, S. O'Brien, L. E. Brus, and T. F. Heinz, Phys. Rev. Lett. **96**, 167401 (2006).
[11] O. Dubay, G. Kresse, and H. Kuzmany, Phys. Rev. Lett. **88**, 235506 (2002).
[12] S. Reich, C. Thomsen, and J. Maultszch, *Carbon Nanotubes: Basic Concepts and Physical Properties*, 1st ed. (Wiley-VCH, Weinheim, 2004), p. 168.
[13] C. Jiang, K. Kempa, J. Zhao, U. Schlecht, U. Kolb, T. Basché, M. Burghard, and A. Mews, Phys. Rev. B **66**, 161404(R) (2002).
[14] H. Maune and M. Bockrath, Appl. Phys. Lett. **89**, 173131 (2006).
[15] V. G. Hadjiev, M. N. Iliev, S. Arepalli, P. Nikolaev, and B. S. Files, Appl. Phys. Lett. **78**, 3193 (2001).
[16] C. A. Cooper, R. J. Young, and M. Halsall, Composites, Part A **32**, 401 (2001).
[17] Pulickel M. Ajayan, Linda S. Schadler, Cindy Giannaris, and Angel Rubio, Adv. Mater. (Weinheim, Ger.) **12**, 750 (2000).
[18] M. D. Frogley, Q. Zhao, and H. D. Wagner, Phys. Rev. B **65**, 113413 (2002).
[19] M. Lucas and R. J. Young, Phys. Rev. B **69**, 085405 (2004).
[20] A. Thess, R. Lee, P. Nikolaev, H. Dai, P. Petit, J. Robert, C. Xu, Y. H. Lee, S. G. Kim, A. G. Rinzler, D. T. Colbert, G. S. Scuseria, D. Tomanek, J. E. Fischer, and R. E. Smalley, Science **273**, 483 (1996).
[21] S. M. Bachilo, M. S. Strano, C. Kittrell, R. H. Hauge, R. E. Smalley, and R. B. Weisman, Science **298**, 2361 (2002).
[22] A. Jorio, R. Saito, J. H. Hafner, C. M. Lieber, M. Hunter, T. McClure, G. Dresselhaus, and M. S. Dresselhaus, Phys. Rev. Lett. **86**, 1118 (2001).
[23] P. M. Ajayan, L. S. Schadler, C. Giannaris, and A. Rubio, Adv. Mater. (Weinheim, Ger.) **12**, 750 (2000).
[24] S. B. Cronin, A. K. Swan, M. S. Ünlü, B. B. Goldberg, M. S. Dresselhaus, and M. Tinkham, Phys. Rev. Lett. **93**, 167401 (2004).
[25] A. Kis, G. Csányi, J.-P. Salvetat, T.-N. Lee, E. Couteau, A. J. Kulik, W. Benoit, J. Brugger, and L. Forró, Nat. Mater. **3**, 153 (2004).
[26] J.-P. Salvetat, G. A. Briggs, J.-M. Bonard, R. R. Bacsa, A. J. Kulik, T. Stöckli, N. A. Burnham, and L. Forró, Phys. Rev. Lett. **82**, 944 (1999).
[27] A. M. Rao, J. Chen, E. Richter, U. Schlecht, P. C. Eklund, R. C. Haddon, U. D. Venkateswaran, Y.-K. Kwon, and D. Tománek, Phys. Rev. Lett. **86**, 3895 (2001).
[28] M. S. Dresselhaus, G. Dresselhaus, A. Jorio, A. G. Souza Filho, and R. Saito, Carbon **40**, 2043 (2002).